Characterization of an unanticipated indium-sulfur metallocycle complex

Morris, Joshua J.; Nevin, Adam; Cornelio, Joel; Easun, Timothy L.

DOI:
10.1098/rsos.230060

Document Version
Publisher's PDF, also known as Version of record

Citation for published version (Harvard):
Morris, JJ, Nevin, A, Cornelio, J & Easun, TL 2023, 'Characterization of an unanticipated indium-sulfur metallocycle complex', *Royal Society Open Science*, vol. 10, no. 9, 230060. https://doi.org/10.1098/rsos.230060

ROYAL SOCIETY OPEN SCIENCE

royalsocietypublishing.org/journal/rsos

Research

Cite this article: Morris JJ, Nevin A, Cornelio J, Easun TL. 2023 Characterization of an unanticipated indium-sulfur metallocycle complex. *R. Soc. Open Sci.* **10**: 230060. https://doi.org/10.1098/rsos.230060

Received: 18 January 2023
Accepted: 7 August 2023

Subject Category:
Chemistry

Subject Areas:
crystallography/supramolecular chemistry/inorganic chemistry

Keywords:
metallocycles, sulfur complexes, catalysis, indium

Author for correspondence:
Timothy L. Easun
e-mail: t.l.easun@bham.ac.uk

This article has been edited by the Royal Society of Chemistry, including the commissioning, peer review process and editorial aspects up to the point of acceptance.

Electronic supplementary material is available online at https://doi.org/10.6084/m9.figshare.c.6824033.

ROYAL SOCIETY OF CHEMISTRY

THE ROYAL SOCIETY PUBLISHING

Characterization of an unanticipated indium-sulfur metallocycle complex

Joshua J. Morris[1], Adam Nevin[1], Joel Cornelio[1,2] and Timothy L. Easun[1,2]

[1]School of Chemistry, Cardiff University, Park Place, Cardiff CF10 3AT, UK
[2]School of Chemistry, University of Birmingham, Haworth Building, Edgbaston, Birmingham B15 2TT, UK

JC, 0000-0003-2536-1868; TLE, 0000-0002-0713-2642

We have produced a novel indium-based metallocycle complex (**In-MeSH**), which we initially observed as an unanticipated side-product in metal–organic framework (MOF) syntheses. The serendipitously synthesized metallocycle forms via the acid-catalysed decomposition of dimethyl sulfoxide (DMSO) during solvothermal reactions in the presence of indium nitrate, dimethylformamide and nitric acid. A search through the Cambridge Structural Database revealed isostructural zinc, ruthenium and palladium metallocycle complexes formed by other routes. The ruthenium analogue is catalytically active and the **In-MeSH** structure similarly displays accessible open metal sites around the outside of the ring. Furthermore, this study also gives access to the relatively uncommon oxidation state of In(II), the targeted synthesis of which can be challenging. In(II) complexes have been reported as having potentially important applications in areas such as catalytic water splitting.

1. Introduction

There has been significant interest in the synthesis of metallocycle compounds due to their potential in sensing [1–3], catalysis [4], molecular magnetism [5,6] and biological applications [7,8]. Metallocycles have been studied in particular as heterogeneous catalysts with very promising results due to the accessibility of active metal sites and unusual oxidation states often found in these relatively large complexes [9–11]. However, many such compounds are made with rare or precious metals and replacing them with more abundant and cheaper alternatives such as indium has become a necessity [12].

Indium compounds such as indium(III) chloride have been used as catalysts for many organic reactions including the hydroarylation of biaryls and cycloisomerization of cyclohexenylalkynes [13].

Indium(III) fluoride and indium(III) triflate promote the cyanation of aldehydes and Diels–Alder reaction of imines [14,15]. Catalysis by indium(II) compounds is relatively uncommon [16]. In(II) selenide has been employed in two-dimensional semiconductors for the fabrication of thin film cells for optoelectronic applications and for water splitting [17,18]. Furthermore, the In(III) state is thermodynamically favoured so the number of reported In(II) compounds is relatively few [19]. Indeed, in this study we were originally using In(III) nitrate as a precursor in reactions intended to make metal–organic frameworks (MOFs), an area of growing interest [20–26], and were surprised to find an In(II) product formed. The synthesis processes of MOFs is an area of particular interest, but relatively little consideration has been given to identifying the side-products when phase-pure materials are not formed [27,28]. After further investigation, we report herein the synthesis and crystal structure of an intriguing and unexpected indium(II)-methanethiolate complex.

2. Material and methods

Synthesis of the **In-MeSH** metallocycle is based on a traditional solvothermal route commonly used for MOF syntheses. In our first synthesis of **In-MeSH**, we included an aromatic dicarboxylic acid linker with the intention of forming a MOF. Subsequent reactions showed that the presence of this dicarboxylic acid plays no appreciable role in the formation of the product, since **In-MeSH** forms in the analogous reaction without the dicarboxylic acid present.

Dimethyl sulfoxide (DMSO, 1.0 ml) was added to a solution of indium nitrate hydrate (92.0 mg, 0.198 mmol) in dimethylformamide (DMSO, 3.0 ml). To this, 6 M HNO_3 (100 µl) was added, and the resulting solution was heated in a sealed Wheaton vial at 65°C for 17 h. The reaction yielded pale yellow cubic crystals of **In-MeSH**. The as-synthesized crystals were analysed by powder X-ray diffraction (PXRD) and the crystal structure was determined by single-crystal X-ray diffraction (SCXRD). Attempts to optimize the synthesis showed that the reaction will not proceed unless DMF is present.

Single-crystal X-ray diffraction data for **In-MeSH** was collected on an Agilent SuperNova Dual Atlas diffractometer at 150 K using Mo Kα radiation ($\lambda = 0.71073$ Å). Crystals were immersed in Fomblin before being loaded onto a MiTeGen Kapton micromount. Data collection and processing were conducted using CrysAlisPro. Structures were solved via dual-space direct methods using ShelXT and refined by full-matrix least-squares on F2 using ShelXL-2014 within the Olex2 software. All non-hydrogenic atoms were refined anisotropically; hydrogen atoms were assigned using a riding model only. A weighting scheme and absorption corrections were applied to the structure. The PXRD pattern was collected at room temperature on a X'PertPro PANalytical Chiller 59 diffractometer using CuKα radiation ($\lambda = 1.5406$ Å). The sample was loaded onto a zero-background silicon wafer directly from the reaction solution, with excess solvent being wicked away with tissue paper before the measurement.

3. Results

In table 1, analysis by single-crystal X-ray diffraction shows that **In-MeSH** crystallizes in the rhombohedral *R*-3 space group, with unit cell parameters a = b = 17.6632 (9) Å, c = 8.7095 (5) Å, and a unit cell volume of 2353.2 (3) $Å^3$. The metallocycle asymmetric unit comprises two components: an indium ion and two deprotonated methanethiol (CH_3S^-) groups which bridge adjacent indium ions to yield an $In_6(CH_3S)_{12}$ metallocycle (figure 1).

Each indium ion is coordinated to four sulfur atoms, one from each of the four deprotonated methanethiol molecules. These sulfur atoms each bridge two indium ions, giving a metallocycle ring that exhibits a distorted square planar coordination around each indium centre; the S1-In-S2 angle is 97.7°, while the S1-In-S1 angle is 81.9°. Furthermore, viewing the metallocycle along the *c*-axis shows the S1-In-S1 and S2-In-S2 angles to be 174.5° and 178.5° out of the plane of the four coordinated sulfur atoms. The In–S distances in **In-MeSH** are between 2.321 and 2.332 Å, which are shorter than both In(III)–S bonds (typically approx. 2.4–2.5 Å) and In(I)–S bonds (typically approx. 2.7 Å) [29–31]. The In–In distance is 3.214 Å, eliminating the possibility of In–In bonds, typically reported to be 2.7–2.8 Å [16].

We compared these bond lengths and angles of **In-MeSH** with its Ru, Zn and Pd analogues, hereby called **Ru-MeSH**, **Zn-MeSH** and **Pd-MeSH**, respectively (electronic supplementary material, tables S1–S3) [32]. All these metallacycles crystallize in the same *R*-3 space group except for **Zn-MeSH**, which

Table 1. Crystal structure data for **In-MeSH**.

crystal data	
chemical formula	$C_{12}H_{36}In_6S_{12}$
Mr	1254.05
crystal system, space group	Trigonal, *R*-3
temperature (K)	150.01
a, c (Å)	17.6543 (8), 8.7083 (4)
V (Å^3)	2350.5 (2)
Z	3.0
radiation type, λ (Å)	Mo Kα, 0.71073
μ (mm^{-1})	0.90
F (000)	1782.0
Dx (Mg m^{-3})	2.658
Θmin., Θmax. (°)	3.5, 29.1
data collection	
diffractometer	SuperNova-Duo, Atlas diffractometer
absorption correction	Multi-scan CrysAlisPro SCALE3 ABSPACK
Tmin., Tmax.	0.933, 1.0000
measured reflections	4331
independent reflections	1326 [$R_{int} = 0.0209$, $R_{sigma} = 0.0233$]
reflections with I > 2σ(I)	1225
refinement	
R[F2 > 2σ(F2)]	0.0240
wR(F2)	0.1071
S	1.12
data/restraints/parameters	1326/0/48
hydrogen treatment	H-atom parameters constrained
largest diff. peak/hole (e Å^{-3})	0.82/−0.58

belongs to the $P2_1/n$ space group. **In-MeSH**, **Ru-MeSH** and **Pd-MeSH** show very similar unit cell lengths (a = b ≈ 17.6–17.8 Å and c = 8.7 Å). For all four of these metallacycles, the M–S bond lengths (approx. 2.3 Å) and M–M distances (approx. 3.1 Å) are also relatively similar (electronic supplementary material, figure S1). In reported structures containing M–M bonds, we observe example bond lengths for Ru–Ru, Zn–Zn and Pd–Pd bonds to be 2.848, 2.358 and 2.6–2.7 Å, respectively [33–35]. Comparing these bond lengths with the M–M distances of the respective metallocycles leads us to conclude that the four metallacycles do not possess M–M bonding.

4. Discussion

The synthesis forms a solid product, within which crystals of sufficient quality to obtain the single crystal structure were identified. However, we also simulated a PXRD pattern from the SCXRD structure and compared it with the experimental pattern of the bulk powder material (figure 2) to find that **In-MeSH** does not form as a phase-pure solid. Peaks at $2\theta = 10.1°$, 15.2°, 18.3°, 20.2°, 26.6° and 39.8° match those reflections simulated from the SCXRD structure, but comparison of the additional observed peaks against indium nitrate hydrate, indium sulfide, cubic and rhombohedral indium oxides, and indium oxyhydroxide did not afford any matches [36]. We suspect that the relatively uncommon In(I) or In(II) oxides may be formed as the other phase in this reaction [37–39] but could not source crystal structures or powder diffraction patterns for either. Furthermore, while the

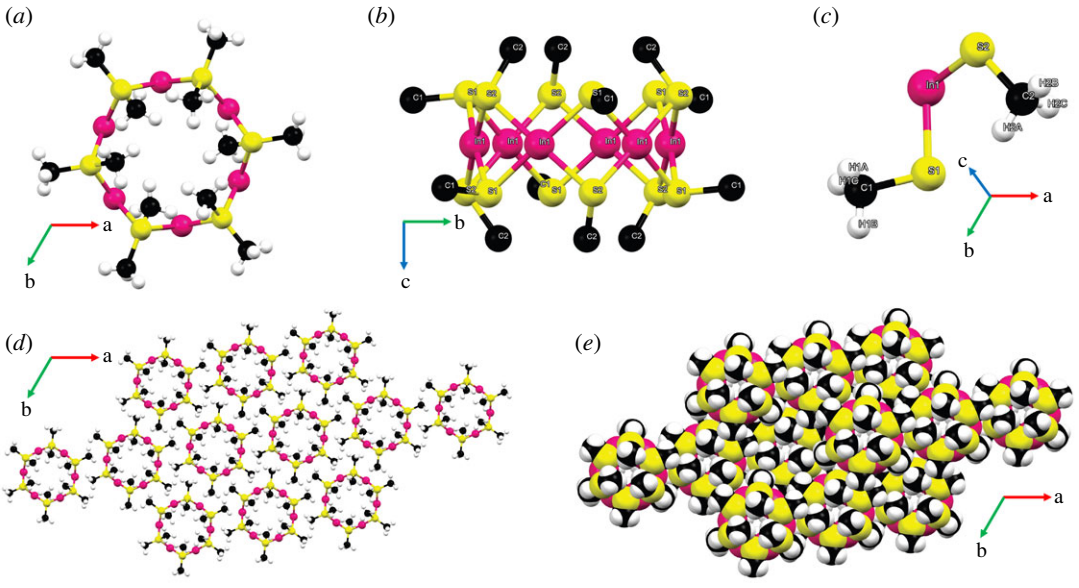

Figure 1. (*a*) The metallocycle viewed along the *c*-axis. (*b*) The metallocycle viewed along the *a*-axis, with the atom labels shown and hydrogen atoms removed for clarity. (*c*) The asymmetric unit. (*d*) Two-dimensional packing viewed along the *c*-axis. (*e*) Space filling diagram of **In-MeSH** showing no voids. Colour code: pink: indium, yellow: sulfur, black: carbon, white: hydrogen.

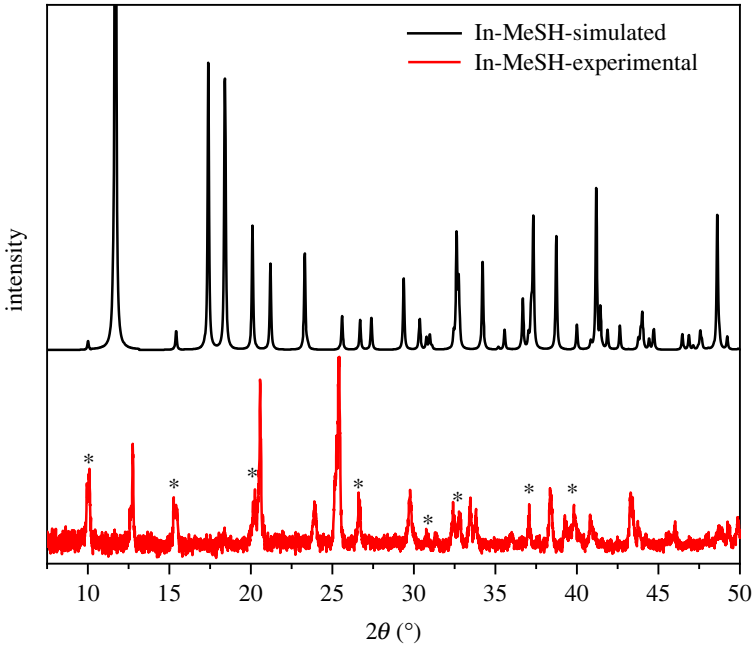

Figure 2. A comparison of the PXRD pattern of synthesized **In-MeSH** (red) to the PXRD simulated from the SCXRD (black). Asterisks indicate peaks that match with the simulated PXRD.

precursor indium nitrate hydrate no longer appears to be present, there may be solid unreacted indium nitrate present as a different solvate than at the start of the reaction.

The analogous Ru complex has an absorption band at 365 nm ascribed to an ligand-to-metal charge transfer (LMCT) transition [32]. This LMCT band tails off in the blue region, around 420 nm, which gives the Ru-complex a yellow colour. For **In-MeSH**, while the metal-based orbitals will certainly be different, if the lowest unoccupied molecular orbital (LUMO) is primarily metal-based across the indium ions, a charge transfer transition may again be the source of the pale-yellow colour observed for these crystals [40]. A full spectroscopic characterization was unfortunately not possible with the limited amount of material available but efforts are underway to make phase-pure **In-MeSH** and perform both experimental and computational characterization of its optical and electronic properties.

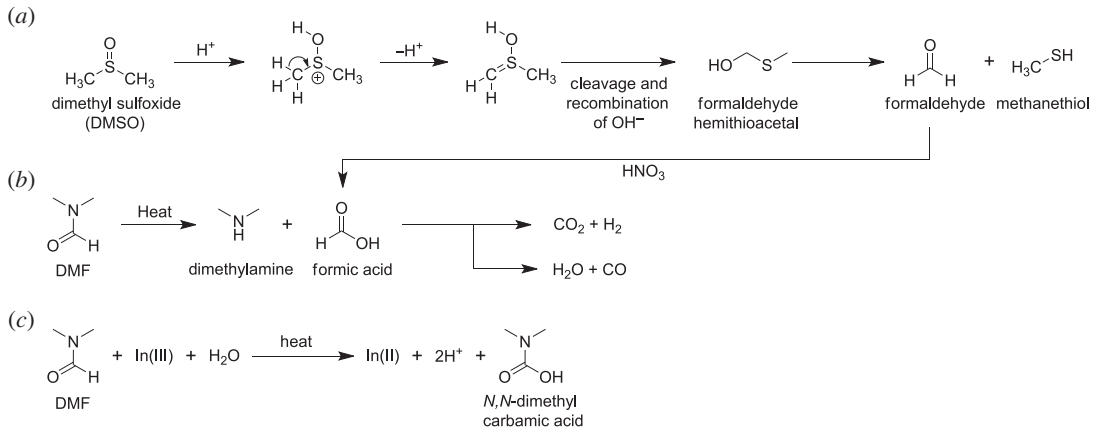

Figure 3. (*a*) Acid catalysed decomposition of DMSO generates methanethiol *in situ*, which subsequently binds to In(II) ions to form **In-MeSH**; (*b*) DMF thermally decomposes, forming hydrogen or carbon monoxide which in turn could reduce In(III) to In(II); (*c*) DMF oxidation to *N,N*-dimethyl carbamic acid could simultaneously reduce In(III) to In(II).

As **In-MeSH** contains methanethiol, which was not one of the initial reactants, the solvothermal conditions used must generate methanethiol *in situ*. If this is a slow or low-yielding process, that may explain the observed low yield and phase-impure solid product. The decomposition of DMSO into methanethiol (figure 3*a*) via an acid-catalysed Pummerer rearrangement has been well studied [30,41–43]. In the presence of strong acids such as HNO_3, DMSO forms formaldehyde hemithioacetal, which decomposes to methanethiol and formaldehyde. We propose that this is the source of the methanethiol which reacts with In(II) ions, the origin of which are discussed below.

The 2+ oxidation state of the indium ions was determined by inspection of the asymmetric unit, which consists of one indium ion and two methanethiol molecules, each of which formally contributes a 1− charge. It is notable that the reaction only proceeds in the presence of DMF and hence we suspect that DMF is responsible for the reduction of indium (III) to indium (II). Though we could not find specific literature for the DMF reduction of In(III) to In(II), the utility of DMF for the reduction of metal ions is well known, with reported examples including the reduction of Au(III) to Au(0), Ag(I) to Ag(0), W(VI) to W(IV), Pd(II) to Pd(0) and, most pertinently given the existence of an analogous isostructural ruthenium metallocycle, Ru(III) to Ru(II) [44–51]. As suggested by Nagata & Obora, under heating DMF could react via two methods: (i) thermal breakdown via formic acid into either water and carbon monoxide (figure 3*b*) or carbon dioxide and hydrogen, the latter of which in both cases serves as the reducing species, or (ii) DMF reduces the In(III) to In(II), being oxidized to *N,N*-dimethyl carbamic acid in the process (figure 3*c*) [45]. Our reaction medium is strongly acidic, in principle inhibiting the second of these options. As a third alternative, formaldehyde generated from decomposition of DMSO (figure 3*a*) could also be oxidized by HNO_3 to formic acid, potentially providing another route to reducing In(III) to In(II), but the absence of **In-MeSH** formation when DMF is not present makes this appear a less likely pathway.

The metallocycle itself, it is worth noting, has no pores or voids capable of storing any residual molecules of the solvents DMF or DMSO. Packing in the crystal structure appears to be via weak van der Waals interactions and no stronger supramolecular interactions are apparent. We have compared the crystal structure of **In-MeSH** with its zinc, ruthenium and palladium analogues [32]. As for **In-MeSH**, the Zn(II), Ru(II) and Pd(II) analogues show distortions from the ideal square planar angle of 90° to about 97.7° around each metal centre. The M(II)-S bond length in all four metallocycles is between 2.2 and 2.3 Å. An astute reviewer of this manuscript suggested that perhaps we had made the **Pd-MeSH** analogue as a result of trace Pd-impurities carried through from linker synthesis via cross-coupling reactions. The existence of **Pd-MeSH** forming as a side product in MOF reactions when Pd-catalysed cross-coupling reactions are used for ligand synthesis certainly cannot be ruled out in such cases. The unit cell lengths of the Pd(II) analogue, **Pd-MeSH** are indeed very similar to **In-MeSH** (electronic supplementary material, table S1). However, small differences exist between the S2-M-S2 angles (electronic supplementary material, table S3) and between the M–M distances: 3.214 Å for **In-MeSH** and 3.126 Å in **Pd-MeSH** (electronic supplementary material, figure S1). Since we are able to synthesize **In-MeSH** without any organic ligand present we rule out this possibility.

The Ru analogue is reported to be catalytically active for the alkenylation of aryl pyridines [32]. Though there are not many reports of catalysis by In(II) compounds, we believe that due to the comparatively high abundance of indium in the Earth's crust and the significantly lower cost compared with ruthenium (*ca* 250 times more abundant and *ca* 100 times cheaper) [52,53], **In-MeSH** is a good candidate for future catalyst testing. The catalytic activity of the analogous ruthenium metallacycle is ascribed to the vacant axial coordination site, present again here in the indium-based structure. If obtainable as a phase-pure material, **In-MeSH** may also serve as an effective reducing agent due to the fact that the In(III) state is thermodynamically preferred [19].

5. Conclusion

An unanticipated indium(II)-based metallocycle compound has been synthesized using indium nitrate, DMF, HNO_3 and DMSO. This compound may well be a common side product in many MOF reactions, as it is formed via the partial decomposition of the DMSO solvent in an acidic environment. The unusual metalloband structure contains indium ions in the relatively uncommon 2+ oxidation state and their distorted square-planar geometry means they are potentially accessible by solvents or catalytic substrates in an analogous manner to the previously reported ruthenium structural analogue. Experiments to synthesize phase-pure **In-MeSH** and investigate catalytic activity are underway.

Ethics. This work did not require ethical approval from a human subject or animal welfare committee.

Data accessibility. The crystallographic dataset supporting this article has been uploaded in the electronic supplementary material and has been submitted to the Cambridge Crystallographic Data Centre, reference CCDC 2235845. These data can be obtained free of charge via https://www.ccdc.cam.ac.uk/structures/.

The data are provided in electronic supplementary material [54].

Authors' contributions. J.J.M.: conceptualization, data curation, formal analysis, investigation, methodology, writing—original draft, writing—review and editing; A.N.: conceptualization, data curation, formal analysis, investigation, supervision, validation, writing—original draft, writing—review and editing; J.C.: data curation, formal analysis, investigation, validation, writing—review and editing; T.L.E.: conceptualization, data curation, formal analysis, funding acquisition, methodology, project administration, resources, supervision, writing—original draft, writing—review and editing.

All authors gave final approval for publication and agreed to be held accountable for the work performed therein.

Conflict of interest declaration. There are no competing interests.

Funding. T.L.E. thanks the Universities of Birmingham and Cardiff, and gratefully acknowledges the Royal Society for the award of a University Research Fellowship (6866 and URF\R\201028) and a Challenge Grant (CH160129) which funded J.C. and A.N., respectively.

Acknowledgements. We are thankful to Dr Benson Kariuki (Cardiff University) for collecting the SCXRD data. We are grateful to the reviewers of this manuscript for helpful and insightful reviews, in particular for highlighting the potential role of the **Pd-MeSH** compound discussed above.

References

1. Lim C-S, Jankolovits J, Zhao P, Kampf JW, Pecoraro VL. 2011 Gd(III)[15-metallacrown-5] recognition of chiral α-amino acid analogues. *Inorg. Chem.* **50**, 4832–4841. (doi:10.1021/ic102579t)
2. Jankolovits J, Cutland Van-Noord AD, Kampf JW, Pecoraro VL. 2013 Selective anion encapsulation in solid-state Ln(III)[15-metallacrown-5]$^{3+}$ compartments through secondary sphere interactions. *Dalton Trans.* **42**, 9803–9808. (doi:10.1039/C3DT50535A)
3. Zhang L, Liu H, Yuan G, Han Y-F. 2021 Chiral coordination metallacycles/metallacages for enantioselective recognition and separation. *Chin. J. Chem.* **39**, 2273–2286. (doi:10.1002/cjoc.202100180)
4. Benchimol E, Nguyen B-NT, Ronson TK, Nitschke JR. 2022 Transformation networks of metal–organic cages controlled by chemical stimuli. *Chem. Soc. Rev.* **51**, 5101–5135. (doi:10.1039/D0CS00801J)
5. Ostrowska M, Fritsky IO, Gumienna-Kontecka E, Pavlishchuk AV. 2016 Metallacrown-based compounds: applications in catalysis, luminescence, molecular magnetism, and adsorption. *Coord. Chem. Rev.* **327–328**, 304–332. (doi:10.1016/j.ccr.2016.04.017)
6. Happ P, Plenk C, Rentschler E. 2015 12-MC-4 metallacrowns as versatile tools for SMM research. *Coord. Chem. Rev.* **289–290**, 238–260. (doi:10.1016/j.ccr.2014.11.012)
7. Kelly ME *et al.* 2008 Platinum(IV) metallacrown ethers: synthesis, structures, host properties and anticancer evaluation. *Organometallics.* **27**, 4917–4927. (doi:10.1021/om800323z)
8. Ning Y, Jin G-Q, Wang M-X, Gao S, Zhang J-L. 2022 Recent progress in metal-based molecular probes for optical bioimaging and biosensing. *Curr. Opin. Chem. Biol.* **66**, 102097. (doi:10.1016/j.cbpa.2021.102097)
9. Mezei G, Zaleski CM, Pecoraro VL. 2007 Structural and functional evolution of metallacrowns. *Chem. Rev.* **107**, 4933–5003. (doi:10.1021/cr078200h)
10. Song L-C, Gao J, Wang H-T, Hua Y-J, Fan H-T, Zhang X-G, Hu Q-M. 2006 Synthesis and structural characterization of metallocrown ethers containing butterfly Fe_2S_2 Cluster Cores. Biomimetic Hydrogen Evolution Catalyzed by $Fe_2(\mu\text{-}SCH_2CH_2OCH_2CH_2S\text{-}\mu)(CO)_6$. *Organometallics* **25**, 5724–5729. (doi:10.1021/om060711r)
11. Mullins CS, Pecoraro VL. 2008 Reflections on small molecule manganese models that seek to mimic photosynthetic water oxidation chemistry. *Coord. Chem. Rev.* **252**, 416–443. (doi:10.1016/j.ccr.2007.07.021)
12. National Research Council. 2012 *The role of the chemical sciences in finding alternatives to*

critical resources: a workshop summary. Washington, DC: The National Academies Press.
13. Davenel V, Puteaux C, Nisole C, Fontaine-Vive F, Fourquez J-M, Michelet V. 2021 Indium-catalyzed cycloisomerization of 1,6-cyclohexenylalkynes. *Catalysts* **11**, 546. (doi:10.3390/catal11050546)
14. Das S, Rawal P, Bhattacharjee J, Devadkar A, Pal K, Gupta P, Panda TK. 2021 Indium promoted C(sp3)–P bond formation by the Domino A3-coupling method – a combined experimental and computational study. *Inorg. Chem. Front.* **8**, 1142–1153. (doi:10.1039/D0QI01210F)
15. Nakanishi K, Jimenez-Halla JOC, Yamazoe S, Nakamoto M, Shang R, Yamamoto Y. 2021 Synthesis and isolation of an anionic bis(dipyrido-annulated) N-heterocyclic carbene CCC-pincer iridium(III) complex by facile C–H bond activation. *Inorg. Chem.* **60**, 9970–9976. (doi:10.1021/acs.inorgchem.1c01236)
16. Pardoe JAJ, Downs AJ. 2007 Development of the chemistry of indium in formal oxidation states lower than +3. *Chem. Rev.* **107**, 2–45. (doi:10.1021/cr068027+)
17. Boukhvalov DW, Gürbulak B, Duman S, Wang L, Politano A, Caputi LS, Chiarello G, Cupolillo A. 2017 The advent of indium selenide: synthesis, electronic properties, ambient stability and applications. *Nanomaterials* **7**, 372. (doi:10.3390/nano7110372)
18. Kishore MRA, Ravindran P. 2017 Te doped indium (II) selenide photocatalyst for water splitting: a first principles study. *AIP Conf. Proc.* **1832**, 090029. (doi:10.1063/1.4980582)
19. Grocholl L, Schranz I, Stahl L, Staples RJ. 1998 Syntheses and molecular structures of bis(tert-butylamido)cyclodiphosph(III)azane cage complexes of thallium(I) and indium(II). *Inorg. Chem.* **37**, 2496–2499. (doi:10.1021/ic9716316)
20. Tansell AJ, Jones CL, Easun TL. 2017 MOF the beaten track: unusual structures and uncommon applications of metal–organic frameworks. *Chem. Cent. J.* **11**, 100. (doi:10.1186/s13065-017-0330-0)
21. Savage, M. *et al*. 2016 Selective adsorption of sulfur dioxide in a robust metal–organic framework material. *Adv. Mater.* **28**, 8705–8711. (doi:10.1002/adma.201602338)
22. Haddad J, Whitehead GFS, Katsoulidis AP, Rosseinsky MJ. 2017 In-MOFs based on amide functionalised flexible linkers. *Faraday Discuss.* **201**, 327–335. (doi:10.1039/C7FD00085E)
23. Grigoropoulos A. *et al*. 2016 Encapsulation of an organometallic cationic catalyst by direct exchange into an anionic MOF. *Chem. Sci* **7**, 2037–2050. (doi:10.1039/C5SC03494A)
24. Ha PTM, Lieu TN, Doan SH, Phan TTB, Nguyen TT, Truong T, Phan NTS. 2017 Indium-based metal–organic frameworks as catalysts: synthesis of 2-nitro-3-arylimidazo[1,2-a]pyridines via oxidative amination under air using MIL-68(In) as an effective heterogeneous catalyst. *RSC Adv.* **7**, 23 073–23 082. (doi:10.1039/C7RA02802D)
25. Carrington EJ, McAnally CA, Fletcher AJ, Thompson SP, Warren M, Brammer L. 2017 Solvent-switchable continuous-breathing behaviour in a diamondoid metal–organic framework and its influence on CO_2 versus CH_4 selectivity. *Nat. Chem.* **9**, 882–889. (doi:10.1038/nchem.2747)
26. Carrington EJ, Dodsworth SF, van Meurs S, Warren MR, Brammer L. 2021 Post-synthetic modification unlocks a 2D-to-3D switch in MOF breathing response: a single-crystal-diffraction mapping study. *Angew. Chem. Int. Ed.* **60**, 17 920–17 924. (doi:10.1002/anie.202105272)
27. Jones CL, Hughes CE, Yeung HHM, Paul A, Harris KDM, Easun TL. 2021 Exploiting in situ NMR to monitor the formation of a metal–organic framework. *Chem. Sci.* **12**, 1486–1494. (doi:10.1039/D0SC04892E)
28. Cerasale DJ, Ward DC, Easun TL. 2022 MOFs in the time domain. *Nat. Rev. Chem.* **6**, 9–30. (doi:10.1038/s41570-021-00336-8)
29. Suh S, Hoffman DM. 1998 Indium tris(alkylthiolate) compounds. *Inorg. Chem.* **37**, 5823–5826. (doi:10.1021/ic980671m)
30. Řičica T, Milasheuskaya Y, Růžičková Z, Němec P, Švanda P, Zmrhalová ZO, Jambor R, Bouška M. 2019 Synthesis and application of monomeric chalcogenolates of 13 group elements. *Chem.: Asian J.* **14**, 4229–4235. (doi:10.1002/asia.201901085)
31. Yurkerwich K, Buccella D, Melnick JG, Parkin G. 2008 Monovalent indium in a sulfur-rich coordination environment: synthesis, structure and reactivity of tris(2-mercapto-1-tert-butylimidazolyl)hydroborato indium, [TmBut]In. *Chem. Commun.* 3305–3307. (doi:10.1039/B803037E)
32. Xie M-H, Wang M, Wu C-D. 2009 Catalytic alkenylation of phenylpyridines with terminal alkynes by a [12]metallacrown-6 ruthenium(II) compound. *Inorg. Chem.* **48**, 10 477–10 479. (doi:10.1021/ic901309b)
33. Clucas WA, Armstrong RS, Buys IE, Hambley TW, Nugent KW. 1996 X-ray crystallographic study of the ruthenium blue complexes $[Ru_2Cl_3(tacn)_2](PF_6)_2{\cdot}4H_2O$, $[Ru_2Br_3(tacn)_2](PF_6)_2{\cdot}2H_2O$, and $[Ru_2I_3(tacn)_2](PF6)_2$: steric interactions and the Ru—Ru 'bond length'. *Inorg. Chem.* **35**, 6789–6794. (doi:10.1021/ic9605377)
34. Wang Y *et al.* 2005 On the chemistry of Zn—Zn bonds, RZn—ZnR (R=[{(2,6-$Pri_2C_6H_3$)N(Me)C}$_2$CH]): synthesis, structure, and computations. *J. Am. Chem. Soc.* **127**, 11 944–11 945. (doi:10.1021/ja053819r)
35. Walensky JR, Fafard CM, Guo C, Brammell CM, Foxman BM, Hall MB, Ozerov OV. 2013 Understanding Pd–Pd bond length variation in (PNP)Pd–Pd(PNP) dimers. *Inorg. Chem.* **52**, 2317–2322. (doi:10.1021/ic301629m)
36. Sorescu M, Diamandescu L, Tarabasanu-Mihaila D, Teodorescu VS. 2004 Nanocrystalline rhombohedral In_2O_3 synthesized by hydrothermal and postannealing pathways. *J. Mater. Sci.* **39**, 675–677. (doi:10.1023/B:JMSC.0000011529.01603.fc)
37. Hinchcliffe AJ, Ogden JS. 1973 Matrix isolation studies on the gallium-indium-oxygen system: infrared spectra and structures of molecular gallium(I) oxide, indium(I) oxide and indium gallium suboxide (InOGa). *J. Phys. Chem.* **77**, 2537–2544. (doi:10.1021/j100907a010)
38. Burkholder TR, Yustein JT, Andrews L. 1992 Reactions of pulsed laser evaporated gallium and indium atoms with molecular oxygen: matrix infrared spectra of new gallium dioxide and indium dioxide species. *J. Phys. Chem.* **96**, 10 189–10 195. (doi:10.1021/j100204a019)
39. Andrews L, Kushto GP, Yustein JT, Archibong E, Sullivan R, Leszczynski J. 1997 Reactions of pulsed-laser-evaporated thallium atoms with O_2: matrix infrared spectra of new TlO_2 species: trends in group 13 dioxides and dioxide anions. *J. Phys. Chem. A.* **101**, 9077–9084. (doi:10.1021/jp9723325)
40. Tai Y-X, Ji Y-M, Lu Y-L, Li M-X, Wu Y-Y, Han Q-X. 2016 Cadmium(II) and indium(III) complexes derived from 2-benzoylpyridine N(4)-cyclohexylthiosemicarbazone: Synthesis, crystal structures, spectroscopic characterization and cytotoxicity. *Synth. Met.* **219**, 109–114. (doi:10.1016/j.synthmet.2016.05.015)
41. Santosusso TM, Swern D. 1974 Acid catalysis as a basis for a mechanistic rationale of some dimethyl sulfoxide reactions. *Tetrahedron Lett.* **15**, 4255–4258. (doi:10.1016/S0040-4039(01)92135-5)
42. Bollyn M. 2006 DMSO can be more than a solvent: thermal analysis of Its chemical interactions with certain chemicals at different process stages. *Org. Process Res. Dev.* **10**, 1299–1312. (doi:10.1021/op060158p)
43. Deguchi Y, Kono M, Koizumi Y, Izato Y-I, Miyake A. 2020 Study on autocatalytic decomposition of dimethyl sulfoxide (DMSO). *Org. Process Res. Dev.* **24**, 1614–1620. (doi:10.1021/acs.oprd.0c00113)
44. Heravi MM, Ghavidel M, Mohammadkhani L. 2018 Beyond a solvent: triple roles of dimethylformamide in organic chemistry. *RSC Adv.* **8**, 27 832–27 862. (doi:10.1039/C8RA04985H)
45. Nagata T, Obora Y. 2020 N,N-dimethylformamide-protected single-sized metal nanoparticles and their use as catalysts for organic transformations. *ACS Omega.* **5**, 98–103. (doi:10.1021/acsomega.9b03828)
46. Muzart J. 2009 N,N-dimethylformamide: much more than a solvent. *Tetrahedron.* **65**, 8313–8323. (doi:10.1016/j.tet.2009.06.091)
47. Juris A, Balzani V, Barigelletti F, Campagna S, Belser P, von Zelewsky A. 1988 Ru(II) polypyridine complexes: photophysics, photochemistry, electrochemistry, and chemiluminescence. *Coord. Chem. Rev.* **84**, 85–277. (doi:10.1016/0010-8545(88)80032-8)
48. Alsindi WZ, Easun TL, Sun XZ, Ronayne KL, Towrie M, Herrera J-M, George MW, Ward MD. 2007 Probing the excited states of d^6 metal complexes containing the 2,2′-bipyrimidine ligand using time-resolved infrared spectroscopy. 1. Mononuclear and homodinuclear systems. *Inorg. Chem.* **46**, 3696–3704. (doi:10.1021/ic0623112)
49. Elliott CM, Hershenhart EJ. 1982 Electrochemical and spectral investigations of ring-substituted bipyridine complexes of ruthenium. *J. Am. Chem. Soc.* **104**, 7519–7526. (doi:10.1021/ja00390a022)
50. Easun TL, Alsindi WZ, Towrie M, Ronayne KL, Sun X-Z, Ward MD, George MW. 2008 Photoinduced energy transfer in a conformationally flexible Re(I)/Ru(II) dyad probed by time-resolved

infrared spectroscopy: effects of conformation and spatial localization of excited states. *Inorg. Chem.* **47**, 5071–5078. (doi:10.1021/ic702005w)

51. Easun TL, Alsindi WZ, Deppermann N, Towrie M, Ronayne KL, Sun X-Z, Ward MD, George MW. 2009 Luminescence and time-resolved infrared study of dyads containing (diimine)Ru(4,4′-diethylamido-2,2′-bipyridine)$_2$ and (diimine)Ru(CN)$_4$ moieties: solvent-induced reversal of the direction of photoinduced energy-transfer. *Inorg. Chem.* **48**, 8759–8770. (doi:10.1021/ic900924w)
52. Rumble JR, Lide DR, Bruno TJ. 2019 *CRC handbook of chemistry and physics: a ready-reference book of chemical and physical data (2019–2020)*, 100th edn. Boca Raton, FL: CRC Press.
53. Daily Metal Spot Prices. See https://www.dailymetalprice.com/metalprices.php (accessed 6 January 2023).
54. Morris JJ, Nevin A, Cornelio J, Easun TL. 2023 Characterization of an unanticipated indium-sulfur metallocycle complex. Figshare. (doi:10.6084/m9.figshare.c.6824033)